

Fabrication of the Superferric Cyclotron Gas-stopper Magnet at NSCL at Michigan State University

S. S. Chouhan¹, G. Bollen¹, J. DeKamp¹, M. A. Green¹, D. Lawton², C. Magsig¹,
D. J. Morrissey², J. Ottarson², S. Schwarz² and A. F. Zeller¹

¹Facility for Rare Isotope Beams, MSU, East Lansing, MI 48824

²National Superconducting Cyclotron Laboratory, MSU, E. Lansing, MI 48824

E-mail: chouhan@frib.msu.edu

Abstract. The magnet for the cyclotron gas stopper is a newly designed, large warm-iron superconducting cyclotron sector gradient dipole. The maximum field in the centre (gap = 0.18 m) is 2.7 T. The outer diameter of magnet yoke is 4.0 m, with a pole radius of 1.1 m and $B \cdot \rho = 1.8$ T m. The fabrication and assembly of the iron return yoke and twelve pole pieces is complete. Separate coils are mounted on the return yokes that have a total mass of about 167 metric tons of iron. This paper illustrates the design and the fabrication process for the cyclotron gas-stopper magnet that is being fabricated at MSU.

1. Introduction

Rare Isotope Beams (RIBs) are routinely produced from heavy-ions accelerated up to ~ 150 MeV/u by the coupled superconducting cyclotrons (K500 and K1200) at National Superconducting Cyclotron Laboratory (NSCL) by reactions in a thin production target (projectile fragmentation). The RIBs are separated in-flight by the A1900 Fragment Separator, and delivered to various experimental areas [1]. Increasing demands for high-quality, low-energy RIBs for nuclear physics and nuclear astrophysics programs have resulted in the construction of a fragment thermalization system coupled to re-accelerator facility, “ReA”, to provide exotic low energy RIBs (at keV-energies) [2]. The stopped radioactive ions will also feed an ongoing program centred on precision mass measurements of exotic nuclei and laser spectroscopy in addition to delivery to ReA for reacceleration (presently ~ 2 and eventually ~ 15 MeV/u). The fast beams have been slowed down in solid degraders and thermalized in linear helium-filled gas cells. A novel concept to stop the fast beams in a gas-filled reverse cyclotron magnet is being pursued that will avoid many limitations of linear gas cells [3]. The fabrication and assembly of the high performance superferric cyclotron gas stopper magnet for this project with a central field of 2.7 T and a strong focusing gradient with field index below the critical value of $k = -0.2$ is nearly complete and described in this paper.

2. Magnet Design Overview

The cyclotron gas-stopper magnet is a vertical superconducting split-solenoid configured into a focusing dipole with 120° radial symmetry. The magnet poles are divided into three hill and three valley regions. The magnet field profile along a given radius is dominated by the shape of the pole face. The coil cross-section, iron yoke and size were optimized for an operating field of 2.7 T field at an exciting current of 200 A. Table 1 provides the design parameters of the magnet. The coils were wound and shimmed into two separate helium vessels made out of 304 stainless steel and attached to separate yokes. The two coils and yoke assemblies can be opened and will have a warm electrical

connection. Because the magnet has to operate on a high-voltage platform at 60 kV (to extract thermalized RIBs), each coil is cooled by three two-stage pulse-tube cryo-coolers rated at 1.5 W at 4.2 K. The intermediate heat shield surrounding the cold vessel is cooled by a separate liquid nitrogen supply. An active quench protection system will be used to protect the magnet with an external fast dump resistor circuit. Each coil is also equipped with a cold quench protection circuit using diodes and a resistor assembly (at 4K) to protect the coils against a failure of the HTS current leads. The support system for each cold mass consists of six axial compression links (60 degree apart) and three radial tension links that carry the weight of the cold mass. One side of the magnet structure is fixed and the other is placed on a rail system. The rail system for the moveable half provides access to the beam chamber for service purposes. The detailed magnet design has been published previously [4], [5].

Table 1. Design parameters for the cyclotron gas-stopper magnet.

Parameter	Units	Value
Pole Diameter	m	2.20
Return Yoke Outer Diameter	m	4.00
Minimum vertical Gap	mm	180
Maximum Field	T	2.70
Coil Current Density	A/mm ²	55.0
Peak Field in the Coil	T	2.05
Peak Stored Energy at Operating Current	MJ	3.56

3. Fabrication and assembly

3.1. Pole, Return Yoke And Supporting Structure

The yoke and the pole tips are made up of low carbon iron (AISI 1018 and AISI 1006), respectively. After machining the flat backs of the twelve pole tip blocks, a gradient surface was cut with a CNC milling machine at the NSCL. Before removal from the machine a coordinate measuring machine (CMM) was used to compare every other pole piece to the design specifications. For measurement purposes, each pole was divided into sections as shown in figure 1, and a series of measurements were performed. Figure 2 shows the results of the measurement of Section -2 of Hill-1. A total of 248 measurements points were made of this section. The calculated mean-difference and its standard deviation are 0.008 mm and 0.033 mm, respectively. Ninety-nine percent of the data points lie within a normal distribution and fall well-within the specified machining tolerance (± 0.201 mm), as shown by the red lines in figure 2. The six poles for one yoke of the sector magnet are shown hanging from a mounting fixture in figure 3.

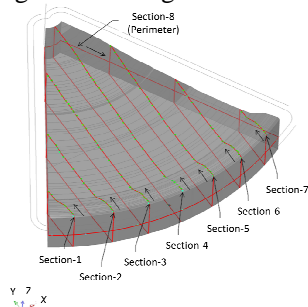


Figure 1. Each pole profile is divided into sections along the radial axis.

Each half of the return yoke consists of major three parts: a lower crescent, a middle slab and an upper crescent, and six return-yoke inserts near the median plane. These pieces were machined at the

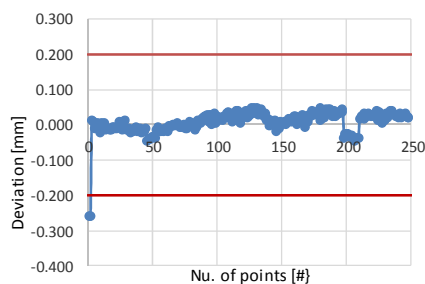


Figure 2. CMM measured data along the radial axis, red horizontal lines indicate the specified tolerance.

supplier from cast iron to the final shape and size. Inspections with a pulsed ultrasonic reflection instrument (Olympus-NDT, model EPOCH-XT) and per ASTM A609, Criteria level III were performed to assure that there weren't any voids in the material. All pole and return yoke pieces were completed by the end of 2012. An end-view of the assembled return yoke structure is shown in figure 4. The entire system is mounted on high voltage stand-off posts. The structure has been hi-potted to the desired level (60 kV) without breakdown. The moveable half of the magnet (~100 tons) is on cradle-shaped support system mounted on six Hilman Rollers® rated at 37.5 tons each [5] that move along hardened steel rails. A small 1 HP (1750 RPM) motor with a small torque of only 2 N-m is used to open and close the whole system.



Figure 3. Machined and assembled hill and valley poles attached to a mounting fixture.



Figure 4. Assembled structure of the return yoke on G-10 posts and the moving-track system.

3.2. Coil/ Cryostat And Cooling System

The cold mass that encloses each superconducting coil has been assembled, tested and welded shut. Three coils were wound, with the third one as a spare. The average diameter of the full coil is 2470 mm and the cross-section is 80 mm by 80 mm. The cross-section of the Formvar™-insulated superconductor in the coil is 1.25 mm by 2.5 mm and the copper-to-superconductor ratio is 4.5. There are 31 turns per layer and 57 layers. The total number of turns in each coil is 1760 and the length of the conductor per coil is 13.8 km. These coils were wet wound with fibre-glass cloth (0.2 mm thick) placed between the layers and baked after winding. The insulation of the conductor is sufficient to withstand the calculated 20 V potential that would occur between layers in a quench. A photograph of two finished coils is shown in figure 5. Each coil was shimmed into the helium vessel with wedge-shape stainless steel and G-10 spacers on the outer radius to supply pre-load. The total stored energy in the magnet is 3.56 MJ and an active quench protection system will be used to protect the magnet.



Figure 5. Completed pair of solenoid coils after removal from the winding form and baking.



Figure 6. Detail of the shimmed coil in the helium vessel and the diode-resistor assembly.

Each coil is also protected from any failure of current leads by back-to-back cold diodes and a resistor assembly across the coil. The cold diode assembly is located in the neck of the helium vessel near the coil and the resistor is a Kapton™-wrapped 6061 aluminium conductor (1 mm by 3 mm cross-section) that is wound on the outer radius of the coil. Measurements of the diode assembly show a forward voltage at a liquid helium temperature of 10 V. To further protect the magnet, an external slow dump (6 V) circuit in the power supply will be used to discharge the stored energy if the power supply fails.

Figure 6 shows the region where the installed superconducting coil is connected to the back-to-back cold diode assembly and aluminium resistor. A stainless steel cryostat provides the required vacuum and cryogenic environment for each coil. The helium vessel is sufficiently stiff to prevent deflection of cold mass if there are unbalanced magnetic loads due to off-centered radial displacement of the coil. The tension links are made of titanium alloy (Ti 6Al4V ELI) and, typical tension loads on the links are calculated to be 5000 kN plus the weight of the cold mass (1600 kN). Figure 7 shows one of the completely assembled cryostats with the support system and the service box of the magnet. The axial magnetic forces during operation will be directed towards the return yoke and carried by six E-Glass fibre composite tubes in compression on each coil. A series of tests were performed on the tubes and the measured failure load was found to be 270 kN giving a factor of safety of 2.4.

The two superconducting coils will be cooled by six pulse tube cryocoolers. The three coolers on each cryostat operate in parallel and also function as helium re-condensers. Each provides ~1.4 W cooling power at 4.2 K and ~40 W at 40 K. The cold heads and ballast tanks are installed on the cryostat tower as shown in figure 8. The connection between rotary valves and cold heads is made with insulators so that the rotary valves, the high-pressure helium lines, and the compressors can be left at ground potential. The intermediate shield is cooled by flowing nitrogen through a line attached to the copper shield. An extra thermal intercept is added at 40K inside the service box to reduce the heat load to manageable level (<15 W per cooler), connected to the first stage of the cooler. The cold heads are mounted at the top of the cryostat tower in the operating configuration as shown in figure 8 as compared to horizontally during assembly as shown in figure 7.

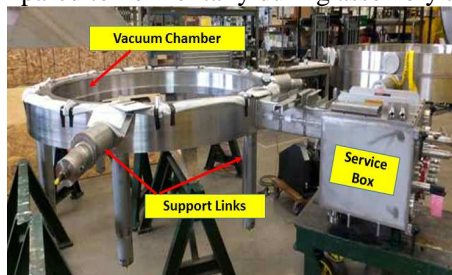


Figure 7. One cryostat assembly shown in the horizontal position upon completion with labels on axial, radial support links and service box.

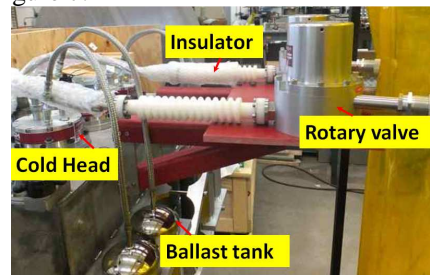


Figure 8. Top of the service box tower showing cold heads and connections during assembly.

4. Summary

Construction of the magnet is in a very advanced state. Fabrication, assembly of the iron structure and both coil cryostats is complete. Extensive testing of the components and instrumentation was carried out during assembly. The initial cool-down and cryogenic testing will be performed once the coil cryostats are mounted in the magnet's iron structure. The operation of the magnet at peak field and field measurements are expected to occur in the first half of 2014.

5. References

- [1] Morrissey DJ et al 2003 *Nuclear Instruments and Methods in Physics Research B* **204** 90.
- [2] Kester O et al 2009 *Proc. Int. Conf. RF Superconductivity* (Berlin, Germany) MOOCAU05.
- [3] Bollen G et al 2005 *Nuclear Instruments and Methods in Physics Research A* **550** 27.
- [4] Chouhan S et al 2013 *IEEE Trans. Appl. Supercond.* **23** 4101805.
- [5] Chouhan S et al 2007 *Proc. IEEE Particle Accelerator Conference PAC-07* 524.
- [6] Hilman Rollers 21150 Butteville Rd NE Donald OR 97020 [Online]. Available: www.hilmanroller-mf.com

Acknowledgments: This work was supported in part by National Science Foundation under grant PHY-0958726 and by Michigan State University.